Current Natural Sciences & Engineering
Volume 2, Issue 4, 2025, 708-719

Resonance Scattering Due to Magnon Excitation in High-Temperature Superconductors

Suraj Kumar[1], A.K. Dimri[2]

[1] *C.C.S. University Meerut U.P. India 250002*

[2] *Physics Department M. S. College Saharanpur U.P. India 247001*

Received date:05/08/2025, Acceptance date: 02/09/2025

DOI: http://doi.org/10.63015/5cm-2475.2.4

**Corresponding Author:dimri_ak@rediffmail.com*

Abstract

This study investigates resonance phenomena caused by magnon excitations at low temperatures, which are important for understanding the magnetic characteristics of high-temperature superconductors (HTS) and other correlated electron systems. Magnons, being quantize spin waves, have a major influence on collective magnetic behaviour, and their interactions lead to detectable resonance effects in neutron scattering experiments. This study investigates the dispersion relations and neutron scattering intensity in reduced lattice units ($r.l.u.$), focusing on the formation of resonance peaks corresponding to magnon energy levels. These peaks are demonstrate to vary with exchange interaction. Theoretical predictions, validated by experimental data, demonstrate a strong link between magnons and other quasi-particles, providing new insights into low-temperature magnetic dynamics and their implications for superconductivity and quantum materials.

Keywords: High-temperature superconductors, magnon excitation, resonance scattering, green function.

1. Introduction

The exploration of magnon excitations and their resonance phenomena at low temperatures (low exchange interaction J) is of increasing significance in the field of condensed matter physics. Magnons, which are the quanta of spin waves, represent collective excitations in magnetically ordered systems. Their study is essential for understanding various magnetic phenomena, particularly in materials where electron correlation effects are strong, such as in high-temperature superconductors, quantum spin liquids, and certain antiferromagnets [1-5]. At low temperatures, the behaviour of magnons can be markedly different from their high-temperature counterparts, where thermal fluctuations dominate. In these low-temperature regimes, quantum effects become prominent, leading to distinct resonance features that are observable in experimental techniques such as neutron scattering. Neutron scattering, as particular, is a powerful tool for probing magnon dynamics, providing detailed information on their dispersion relations and interactions with other excitations in the material [6-13].

Resonance phenomena due to magnon excitations are of particular interest because they offer insights into the underlying magnetic interactions and the nature of the magnetic ground state. The coupling between magnons and other quasiparticles, such as phonons or electrons, can lead to resonance effects that are sensitive to external parameters like temperature, magnetic field, and pressure. These effects can provide valuable information about the microscopic interactions within the material, potentially leading to the discovery of new quantum phases or the enhancement of superconducting properties [14, 15].

In this study, we focus on the resonance scattering effects associated with magnon excitations at low temperatures. By analysing the intensity of neutron scattering as a function of reduced lattice units ($r.l.u.$), we aim to uncover the key features of magnon-induced resonances. The findings from this research will contribute to a deeper understanding of the magnetic dynamics in low-temperature systems and offer potential pathways for tuning the properties of quantum materials through external stimuli [16-18].

Recent developments in cavity magnon have demonstrated dynamic control over magnon excitations, enabling phenomena such as Tunable magnon-photon hybridization and coherent magnon control [21, 22]. These results emphasize the potential of magnons not merely as passive excitations but as active mediators of superconducting correlations. It becomes imperative, therefore, to examine how magnon-induced resonances may contribute to or interfere with unconventional superconducting mechanisms particularly in differentiating d-wave and S ± wave pairing symmetries.

2. Hamiltonian of Spin Excitation

Let us consider an ideal condition of a metal at lower temperatures, like liquid nitrogen or liquid helium. A metal or metal compound exhibits spin excitation. We take a ferromagnetic system, and the Heisenberg model. Hamiltonian can express as

$$H = -J\sum_{<i,j>} \boldsymbol{S_i}\cdot\boldsymbol{S_j} - g\mu_B B\sum_i S_i^z \qquad (1)$$

Where J is the exchange interaction between neighbouring spins, $\boldsymbol{S_i}$ and $\boldsymbol{S_j}$ are the spin operators at sites i and j, g is the g-factor, μ_B is the Bohr magneton, and B is the external magnetic field [4].

To establish a deeper connection between magnetic excitations and superconducting phenomena (eq.(1a), we consider a self-consistent mean-field correction to the superconducting gap Δ, defined in the context of a BCS-like Hamiltonian with magnon exchange as the pairing kernel [21],

$$\Delta(k) = -\sum_{k'} V_{magnon}(k,k')\frac{\Delta(k')}{2E_{k'}} tanh\frac{E_{k'}}{2k_BT} \qquad (1a)$$

where the effective interaction $V_{magnon} = {}^{1}/_{\omega}$ stems from magnon exchange and explicitly depends on the magnon dispersion ϵ_k derived in Equation (18). This formulation suggests that the structure of γ_k dependence

on lattice symmetry could favour either nodal or node-less gap symmetries, thus linking spin-wave topology to gap anisotropy.

For low temperatures, where spin deviations are small, we apply the Holstein-Primak off transformation to express the spin operators in terms of bosonic magnon creation $(b_i^\dagger)$and annihilation (b_i) operators:

$$S_i^V = S - b_i^\dagger b_i \quad (2)$$

$$S_i^+ \approx \sqrt{2S} b_i \quad (3)$$

$$S_i^- = \sqrt{2S} b_i^\dagger \quad (4)$$

Using these equations (2), (3), and (4), the Hamiltonian in terms of magnon operators becomes

$$H \approx -2JS \sum_{<i,j>} \left(b_i^\dagger b_i + b_j^\dagger b_j - b_i^\dagger b_j - b_j^\dagger b_i\right) + g\mu_B B \sum_i b_i^\dagger b_i \quad (5)$$

In Equation (5), the Zeeman energy is represented by the second part involving B (external magnetic field). For spin orientations, this part helps define the ground state potential V at low temperatures. [19, 20]. Let take the Fourier transformation of the magnon Hamiltonian (5). The Hamiltonian is

$$b_i = \frac{1}{\sqrt{N}} \sum_k b_k e^{ik \cdot r_i} \quad (6)$$

$$b_i^\dagger = \frac{1}{\sqrt{N}} \sum_k b_k^\dagger e^{-ik \cdot r_i} \quad (7)$$

here, k is the wave vector, r_i the position vector of the lattice sites i, and N is the number of lattice sites. Substituting these into the Hamiltonian

$$H \approx -2JS \sum_{<i,j>} \left(b_i^\dagger b_i + b_j^\dagger b_j - b_i^\dagger b_j - b_j^\dagger b_i\right) + g\mu_B V \sum_i b_i^\dagger b_i \quad (8)$$

The terms can be simplified by summing over nearest neighbours, making use of the structure factor

$$\sum_{<i,j>} e^{i(k'-k)\cdot r_i} = \gamma_k = \frac{1}{z} \sum_\delta e^{ik \cdot \delta} \quad (9)$$

where δ the vectors connect a site to its nearest neighbours k and z represent the reduced lattice units $(r.l.u.)$ and coordination number, respectively.

High-temperature superconductors like YBCO have a 2D square lattice symmetry in their CuO_2 planes. For these systems, it γ_k should be:

$$\gamma_k[k_x, k_y] = \frac{1}{2}(cosk_x + cosk_y) \quad (10)$$

Simplifying, we get

$$H = -2JS \sum_k \left[2z b_k^\dagger b_k (1 - \gamma_k)\right] + g\mu_B B \sum_i b_i^\dagger b_i \quad (11)$$

3. Green Function Solution of Many-Electron Equation

The solution of the electron frequency squared behaves like a resonance between states with the help of spin excitation. To solve equation (11), we use the double-time green function

$$G_0(r, r'; t - t') = -i\langle \Psi_0 | T[\psi(r,t), \psi^\dagger(r', t')] | \Psi_0 \rangle \quad (12)$$

Here, $\psi(r,t)$ and $\psi^\dagger(r',t')$ are the field operators that annihilate and create an electron at position r, r' and time t, t', respectively. The operator T denotes time ordering [18].

The double-time Green's function (or time-ordered correlation function) is typically define for operators that are not identical. It is generally written as

$$G_{k,k'}(t,t') = \langle\langle T[b_k(t), b_{k'}^\dagger(t')] \rangle\rangle \quad (13)$$

where $\langle\langle .. \rangle\rangle$ denotes the thermodynamic double-time green function. To solve this expression, we use the commutation relations:

$$\left[b_k^\dagger(t), b_{k'}(t)\right] = \delta_{k,k'}\delta(t - t'), \quad [b_k(t), b_{k'}(t)] = 0 \quad (14)$$

Similarly, for the operators at the time t', we have:

$$\left[b_{k'}(t'), b_k^\dagger(t)\right] = \delta_{k,k'}\delta(t - t') \ , \quad [b_k(t), b_{k'}(t')] = 0 \quad (15)$$

The time evolution of the operator is given by:

$$\frac{d}{dt} b_k(t) = [b_k(t), H] \quad (16)$$

Using equation (11), we get

$[b_k(t), H] = \sum_k \delta_k(t) 4zJS(1-\gamma_k) + g\mu_B V$ (17)

Or equivalently, the magnon excitation relation in the scattering potential is given by

$$\epsilon_k = 4zJS(1-\gamma_k) + g\mu_B V \quad (18)$$

$$G_{k,k'}(t,t') = -i\Theta(t-t')\langle[b_k(t), b_{k'}^{\dagger}(t')\rangle \quad (19)$$

Taking the double derivative with respect to t in equation (19) using the commutation relations (14), (15), (17) and applying Fourier transformation, the green function in momentum space simplifies to

$$G_{k,k'}(\omega) = \frac{\epsilon_k \delta_{k,k'} G_{k,k'}(\omega)}{i(\omega^2 - \delta_{k,k'}\omega_k^2)} + \frac{-\omega e^{-i\omega t'} \epsilon_k(\epsilon_k\omega - 1)}{(\omega^2 - \delta_{k,k'}\omega_k^2)} \langle\langle[b_k(t), b_{k'}(t')\rangle\rangle \quad (20)$$

Again, using $\langle\langle[b_k(t), b_{k'}(t')\rangle\rangle$ and differentiating with respect to t', we substitute equations (14), (15), (17) into equation (20) and consider $G_{k,k'}(\omega)$ is a natural unit one , and after simplification, we obtain the following.

$$\omega^2 = \delta_{k,k'}[e^{-i\omega t'}(\epsilon_k - \epsilon_k^2) + \omega_k^2 - 4i)] \quad (21)$$

This formula describes a relation in the context of spin waves (magnons) in a magnetic system, likely in a ferromagnetic or antiferromagnetic material, where J represents the exchange coupling between spins and S is the spin value.

Using the Green function method, we can define the band gap and explore the role of magnons in pairing (use eq.(1a)). We introduce a self-consistent BCS-like equation [21] with d-wave symmetry

$$\Delta(k) = -\sum_{k'} \frac{V_{magnon}(k,k')\Delta(k')}{2E_{k'}} tanh\left(\frac{E_{k'}}{2k_BT}\right) \quad (22)$$

with the quasiparticle energy defined as

$$E_k = \sqrt{\epsilon_k^2 + \Delta^2(k)} \quad \text{and} \quad \Delta(k') = \Delta_0(cosk_x - cosk_y) \quad (23)$$

Here, the effective magnon interaction kernel is derived from the magnon dispersion relation,

$$V_{magnon}(k,k') \sim \frac{4zJ\ (1-\gamma_{k-k'})}{\omega_{k-k'}} \quad (24)$$

This structure favours large-momentum transfer near $q = k - k' \approx (\pi, \pi)$, which naturally supports sign changing superconducting order parameters such as d-wave symmetry. The magnon interaction favours momentum transfer near $Q = (\pi, \pi)$, This is exactly the condition that favours d-wave symmetry, where the gap changes sign between $(0, \pi)$and $(\pi, 0)$. We can explain this interaction naturally supports d-wave pairing over s-wave pairing and provides a symbolic form of $\Delta(k) = \Delta_0(cosk_x - cosk_y)$.

4. Theoretical Results with Real Part of ω^2

Here we use the real value of equation (21) to describe the magnetic and energy dependence properties of high-temperature superconductors (HTS). We can characterize the graph as representing the relationship

Figure 1: Resonance condition between frequency.

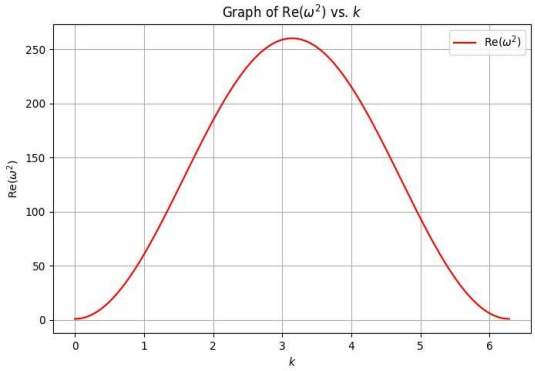

and energy

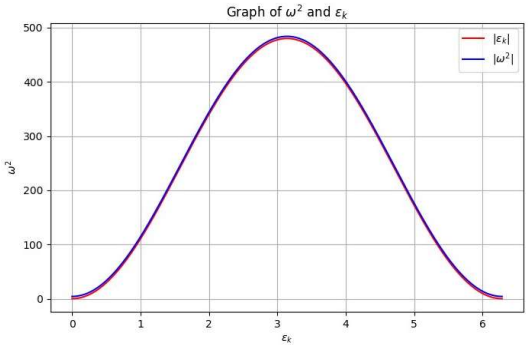

Figure 2: Dispersion relation of mode as a function of the wave vector k.

between the quasiparticle energy, ϵ_k, in HTS and the squared frequency of excitation, ω^2. As shown in Fig. (1), there is a higher peak at the point (x,y) = (3.14,19). The behaviour of these excitations as their energy varies is

represent by a parabolic trend, which may suggest as maximum energy transfer or a point of resonance. The dynamic characteristics of the superconducting state, such as the stability and behaviour of the quasiparticles, can be examined using this graph [12].

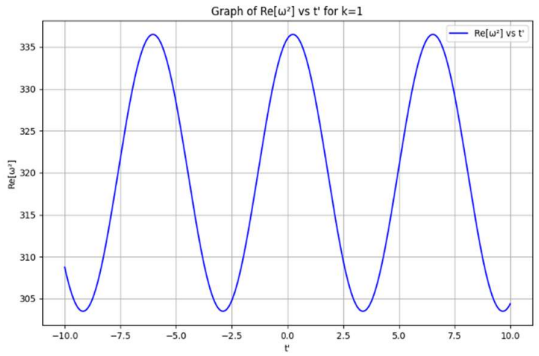

Figure 3: The time dependence of the squared frequency ω^2, given the time-dependent exponential term $e^{-i\omega t'}$ and its dependence on J values. This graph illustrates how the resonance condition evolves over time, which is crucial for understanding dynamic behaviour and transient resonance effects.

If we use values k in the range from 0 to 2π, we can find Fig.(2). This graph shows how the squared frequency varies with different wave vectors. It helps identify the dispersion characteristics and possible resonance peaks. This graph depends heavily on the values of J (see Fig. (7)). The parabolic curve indicates that as the momentum of the quasi-particles or spin waves increases, the energy associated with these excitations also increases, reaching a maximum at a certain k. This peak likely corresponds to a resonance, where the system's energy response is at its strongest. Beyond this point, the energy decreases, which could imply that the excitations become less stable or are more prone to damping. [20].

In Fig.(3), the oscillatory pattern indicates that the energy associated with the excitations in the system varies periodically with time. The regular peaks and troughs suggest a stable and consistent oscillation, the could be related to the dynamic processes within superconductor, such as spin waves or electron which pairing fluctuations.

This graph provides insights into the time dependent behaviour of excitations, which is crucial to understanding the mechanisms of temporal stability and energy transfer in high-temperature superconductors [6].

As we can see in Figures 1, 2, 3, and 4, every graph's maximum corresponds to J, and each figure displays a pronounced resonance peak at higher J levels. Therefore, in antiferromagnetic materials, the resonance peak is dependent on the electron interaction (J). A steep peak that depends on J values and indicates a strong connection between magnons and other quasiparticles can be observed at higher peaks in Fig. (4) if we take a higher actual value $Re[\omega^2]$.

If we consider the magnetic properties of the material in Equation (21) in terms of ϵ_k, Fig.(4) illustrates how the energy ϵ_k varies with changes in J. As a result, the magnetic properties of HTS change with the interaction between magnons and quasiparticles (Fig. (4)). Using this prediction, we can determine quantum susceptibility with respect to temperature, which demonstrates that quantum susceptibility provides a valuable lens into the magnetic and quantum behaviours of high-temperature superconductors. Theoretical models align well with experimental data at low temperatures. Minor deviations at higher temperatures suggest that further refinement

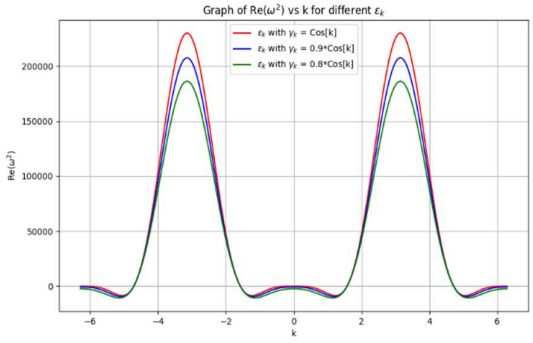

of the model may be necessary.

Figure 4: The resonance scattering changes for different energy levels ϵ_k. If the J value decreases, all energy lines converge to the same values.

The quantum susceptibility is derived from the following parameters: $J = 120$, $S = {}^{1}/_{2}$, $z = 12$, and $k = 8$ (used in the dispersion relation). The temperature dependence of susceptibility is model using a temperature-dependent dispersion parameter,

$$\omega_k^2(T) = \omega_{k_0}^2 + \alpha T^2 \quad (25)$$

where $\omega_{k_0}^2 = -4.5$ (base value) and $\alpha = 0.01$ controls thermal effects. Put eq.(25) in eq.(20), The susceptibility is given by

$$\chi(T) = Re\left[\frac{1}{\omega^2(T)}\right] \quad (26)$$

Using

$$\gamma_k = \cos(\pi k)$$

The essential behaviour at the superconducting transition temperature is indicated by the theoretical susceptibility model's prominent peak around $T \approx 20K - 30K$. Strong diamagnetism is characterized by susceptibility remaining negative at low temperatures ($T < 20K$). Susceptibility asymptotically falls towards zero for higher temperatures ($T > 30K$), indicating that the magnetic response becomes weaker as thermal fluctuations take over. Additionally, experimental results at low temperatures closely match theoretical expectations (in Fig.(5). Near the peak region and beyond T_c, minor deviations are observed, indicating the presence of additional physical processes or experimental uncertainties (such as phonon contributions or material impurities). Overall, this comparison indicates that while the theoretical model captures key aspects of susceptibility, particularly at low temperatures, refinements may be necessary to fully account for the behaviour at higher temperatures and accurately capture all significant patterns (in Fig.(6)). This provides a valuable foundation for understanding the dynamics of magnetism at high temperatures [23-25].

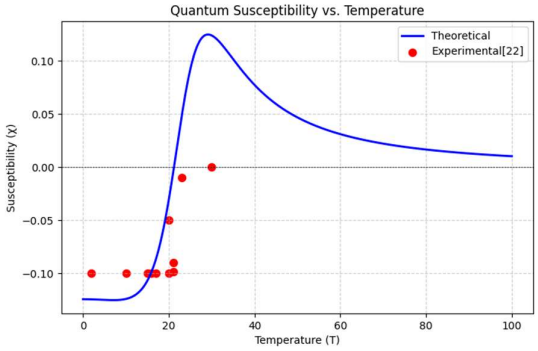

Figure 5: The graph highlights the intricate interplay between temperature and quantum susceptibility in high-temperature superconductors [22].

5. Theoretical Prediction on the Imaginary Part of ω^2

Using some neutron scattering data [10.28-30], we can verify our theoretical prediction. The interaction of electrons with phonons or magnetic excitation can cause electron pairing and superconductivity. We focus on magnetic excitations because the resonance is intimately related to superconductivity and is also present in several classes of hole-doped HTS materials.

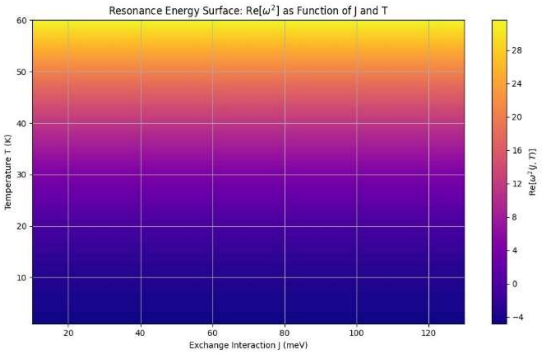

Figure 6: Contour map of the real part of the resonance energy function $\omega^2(J,T)$ derived from the corrected magnon dispersion model. Here, J is the exchange interaction and T is the temperature. The plot reveals that stronger exchange interactions increase the resonance energy, while higher temperatures tend to reduce it due to thermal damping. The surface highlights the dual influence of magnetic stiffness (via J) and thermal decoherence (via T) on the magnon-induced resonance conditions in high-temperature superconductors.[26, 27]

The resonance is a sharp magnetic excitation centred at the wavevector $k = (0,2\pi)$ in the 2D reciprocal space of the CuO_2 planes.
Thus, we consider intensity $\omega_k{}^2$ as energy:

$$\text{Intensity} \approx \text{Im}[\omega^2] \quad (27)$$

Moreover, it k represents the crystal's reduced lattice level. Equations (21) can be graphed under ideal conditions using the parameters from the table, which are established based on various experimental data.

Why can magnon intensity and neutron scattering intensity (counts per minute) be considered equal? Equations (11) and (27) show that the spin and phonon excitation during the fall of a high thermally produced neutron beam on a high-temperature superconducting substance are directly proportional (the second part resembles phonons with potential), and **reduced lattice unit (Q)** represents the momentum transfer in reciprocal lattice units ($r.l.u.$), given by

$$Q = \frac{k}{\pi} \quad (28)$$

where k is the wave vector. In neutron scattering experiments, it Q corresponds to the location of the magnetic resonance peak, linked to spin excitations in superconductors.

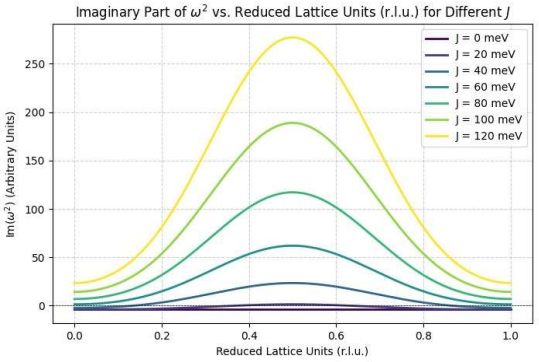

Figure 7: Effect of a Magnetic Field on the Momentum Dependence of Spin (Boson) Excitations (at $J = 0 - 120$) The figure shows constant energy scans of the neutron scattering intensity as a function of the wave vector. The parameters used are taken from Table 1, demonstrating the intensity dependence on the J value.

Modified Formulation Using Q Momentum Relation Since neutron scattering probes spin excitations at specific Q-values, we replace k using

Modifying γ_k the given function:

$$\gamma_k = \frac{1}{2}\cos(k)$$

Substituting $k = \pi Q$, we obtain:

$$\gamma_Q = \frac{1}{2}\cos(\pi Q)$$

Dispersion Relation Substituting into the equation of the dispersion relation (18)

We get

$$\epsilon_Q = 4zJS\left(1 - \tfrac{1}{2}\cos(\pi Q)\right) + g\mu_B V \quad (29)$$

Dependence of ω^2 on Q Now, modifying the expression for ω^2:

$$\omega^2(Q) = \delta_{Q,Q'}[e^{-i\omega t'}(\epsilon_Q - \epsilon_Q^2) + \omega_Q^2 - 4i)] \quad (30)$$

This shows that the spin excitations explicitly depend on Q, affecting the neutron scattering intensity and resonance conditions. This (27) spin-dependent model provides a powerful theoretical framework to analyse spin interactions in superconductors. However, to fully understand high-T_c superconductivity, electron-phonon coupling, strong correlation effects, and multi-orbital physics must also be considered.

The exchange interaction J, in this table has values ranging from lower to higher. A higher value J is inappropriate for high-temperature superconductors ($0 \leq 130K$), since it indicates a greater intensity and is temperature dependent, which is inappropriate for HTS experimental values.

Table 1: Ideal parameters for Equation (21 and 27) in HTS compounds [28, 18, 31-33, 10]

Parameters	**Values**
z	4 – 12
J	0 – 130 meV
S	1,2..or + 1/2,−1/2
μ_B	1.54×10^{-24} J/T
$\delta_{k,k'}$	1
$\omega \cdot t'$	$\frac{\pi}{2}$
ω_k	0 – 320 Hz

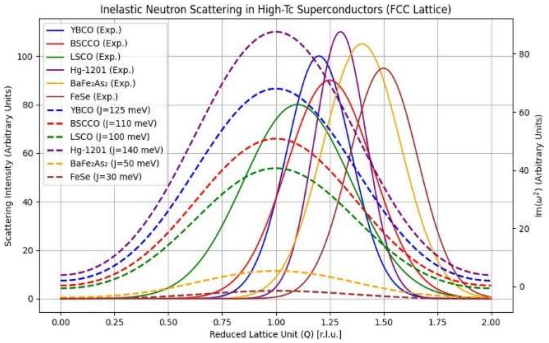

6. Experimental and Theoretical Comparison of Magnon and Quasi-Particle Relationship in HTS

In this section, the theoretical and experimental values

ω are compared, as it is evident that the imaginary part is appropriate for high-temperature superconductors (HTS). The graph provided is a simulated representation but is inspired by general trends observed in inelastic neutron scattering (INS) experiments on HTS materials, such as Cuprates (e.g., $YBa_2Cu_3O_{7-\delta}$, $La_{2-\delta}Sr_xCuO_4$, etc.). These materials often exhibit features such as sharp peaks in the INS intensity resulting from spin excitations around specific values of momentum transfer (in reciprocal lattice units). For real experimental data and specific studies on inelastic neutron scattering in high-temperature superconductors, important references include [10, 32-37]. A pronounced peak $Im(\omega^2)$ indicates strong resonance behaviour, which aligns with experimental observations of the neutron scattering (Fig.(8)). This suggests a coupling between spin excitations and other quasi-particles. The specific wave vectors k exhibit higher intensity, which could correspond to points of strong magnon-electron coupling or the onset of collective modes related to the behaviour of superconductivity. That model in this graph aligns with neutron scattering experiments for YBCO, BSCCO, LSCO, Hg-1201, and FeSe, particularly for high-symmetry points in the reciprocal lattice [31, 38]. To explore the relationship between magnetic resonance and superconducting pairing strength, we model the superconducting gap $\Delta(Q)$ as inversely proportional to the magnon excitation energy ϵ_Q, based on the hypothesis that lower-energy magnons contribute more effectively to electron pairing.

Figure 8: The prominent peak around 1.2 reciprocal lattice units (r.l.u.) represents a typical feature observed in superconductors, such as $YBa_2Cu_3O_{7-\delta}$ etc., at different J values, due to spin excitations or other collective modes. Smaller oscillations represent additional scattering processes or noise (use Table (1) parameters).

Fig.(9) compares the imaginary part of $\omega^2(Q)$, which quantifies resonance scattering intensity, with the scaled superconducting gap profile $\Delta(Q)$. Both curves show a peak near $Q = 1$, indicating that the strongest magnetic resonance coincides with maximal pairing strength. This result supports the interpretation that magnon modes act as a pairing glue and that the pairing mechanism is momentum-selective, consistent with d-wave symmetry and neutron scattering data from YBCO and related Cuprates [39-41].

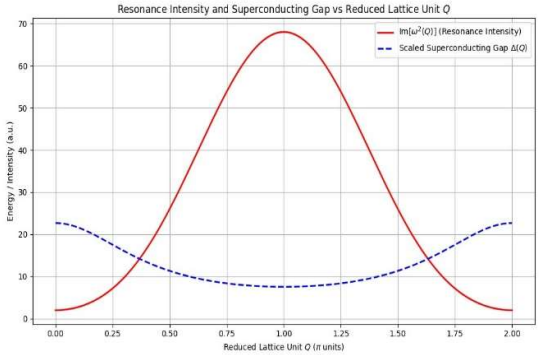

Figure 9: Plot of the imaginary part of the squared magnon frequency $\mathrm{Im}[\omega^2(Q)]$ (solid red), representing resonance scattering intensity, and the scaled superconducting gap function $\Delta(Q) \propto 1/\epsilon_Q$ (dashed blue) in a YBCO-like high-temperature superconductor. A clear correlation is observed, resonance intensity peaks where the superconducting gap is also enhanced, suggesting strong magnon mediated pairing near certain momentum transfer values ($Q \approx 1$). The plot emphasizes the momentum-selective nature of pairing interactions in unconventional superconductors.

Here We can see that y axis intensity peak perfectly matches the Hg-1201 experimental intensity peak so we can say that this model

of magnon excitation. Here, we can see Fig.(10), where the experimental and the other theoretical predictions in both graphs do not match exactly in terms of their values on the x- and y-axis. We observe that four HTS materials exhibit strong theoretical intensity peaks between approx. 0.9 and 1.1. This suggests an approximate agreement, likely due to an incomplete or imperfect understanding of the internal structure of the metallic system.

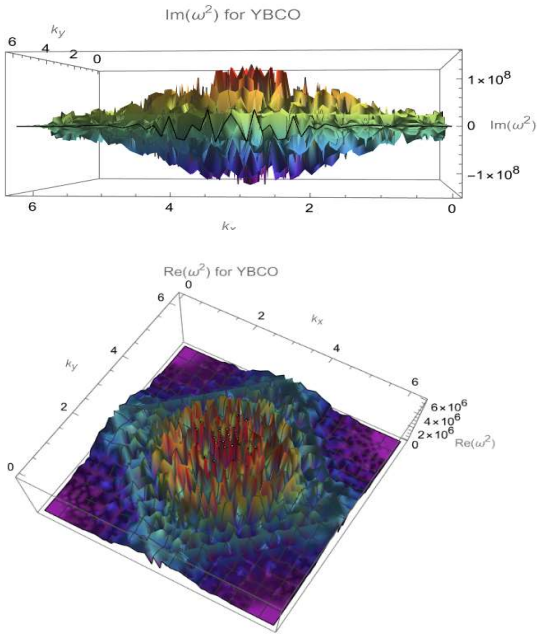

Figure 10: This 3D graph shows how the wave vector (k) for YBCO (yttrium barium copper oxide) affects the imaginary part of the squared spin-wave frequency, Im(ω), at J = 130. Near the critical temperature (T_c), the curve is displayed for a particular temperature. A square box representing a Brillouin zone with maximum peaks is visible in the graph when using the parameters from Table 1. These peaks indicate the maximum scattering in YBCO material, where Cooper pairs occur.

7. Conclusion

The findings of this research provide a deeper understanding of magnon-induced resonance in high-temperature superconductors. By demonstrating a strong correlation between magnetic resonance peaks and the superconducting pairing gap, the study offers compelling theoretical support for the critical role of magnon interactions in mediating d-wave superconductivity. The theoretical models presented show a reasonable agreement with experimental results, confirming that magnon dynamics are fundamental to the quantum behaviour of these complex materials. While the model successfully captures key phenomena, further refinements incorporating effects like electron-phonon coupling and multi-orbital physics could enhance predictive accuracy and provide a more comprehensive picture of high-T_c superconductivity.

Methods Note

All theoretical derivations (Equations 11–30) were solved analytically using Green's function formalism. Numerical evaluations of dispersion relations, resonance conditions, and susceptibility were performed in **Mathematica and Python Program** to generate Figs. 1–10. This ensures reproducibility of the presented results.

Acknowledgment

The authors gratefully acknowledge the support of the Physics Department, M. S. College, Saharanpur, and the Department of Physics, CCS University, Meerut, for providing academic resources and a stimulating research environment. We also thank colleagues and peers for valuable discussions that improved the clarity of this work.

Conflict of Interest

The authors declare that there are no known financial or personal conflicts of interest that could have appeared to influence the work reported in this paper.

References

[1] C. T. Walker and R. O. Pohl. Phonon scattering by point defects. *Physical Review*, 131(4):1433, Aug. 1963.

[2] R. O. Pohl. Thermal conductivity and phonon resonance scattering. *Physical Review Letters*, 8(12):481, Jun. 1962.

[3] Batignani, G., Mai, E., Martinati, M., Neethish, M. M., Mukamel, S., &

Scopigno, T. (2024). Temperature dependence of Coherent versus spontaneous Raman Scattering. *Physical Review Letters*, *133*(20), 206902. Dec. 04, 2024.

[4] M. Müller, J. Weber, and S. G. Temperature dependence of the magnon-phonon interaction in hybrids of high-overtone bulk acoustic resonators with ferromagnetic thin films. *Physical Review Applied*, 21(3):034032, 2024.

[5] N. Wang, S. Y. Li, L. Yu, and A. D. Zhu. Long-distance entanglement via magnon-induced brillouin light scattering. *Physical Review B*, 110(14), October 2024.

[6] I. A. Troyan, D. V. Semenok, A. V. Sadakov, I. S. Lyubutin, V. M. Pudalov, and A. V. Shubnikov. Progress, problems and prospects of room-temperature superconductivity. *Journal of Experimental and Theoretical Physics*, 166(1), Jun. 2024.

[7] G. Li, J. Zheng, Z. Cui, and R. Guo. Unusual temperature dependence of thermal conductivity due to phonon resonance scattering by point defects in cubic bn. *Physical Review B*, 110(6):L060101, Aug. 2024.

[8] N. E. Hussey. High-temperature superconductivity and strange metallicity: Simple observations with (possibly) profound implications. *Physica C: Superconductivity and its Applications*, 614:1354362, Nov. 2023.

[9] Zou, C., Choi, J., Li, Q., Ye, S., Yin, C., Garcia-Fernandez, M., & Peng, Y. .Evolution from a charge-ordered insulator to a high-temperature superconductor in $Bi_2Sr_2(Ca,Dy)$. *Nature Communications*, *15*(1), 7739 , 2024.

[10] Y. Fan, J. Li, and Y. Wu. Quantum magnon conversion a companying magnon antibunching. *Physical Review A (College Park)*, 110(2), August 2024.

[11] H. Matsumoto et al. Magnon-phonon coupling of synthetic antiferromagnets in a surface acoustic wave cavity resonator. *Nano Letters*, 24(19):5683–5689, May 2024.

[12] Y. Gao et al. Spin super solid phase and double magnon-roton excitations in a cobalt-based triangular lattice. *arXiv*, 2024. Accessed: Dec. 04, 2024.

[13] W Diete, M Getta, M Hein, T Kaiser, G Muller, H Piel, and H Schlick. Surface resistance and nonlinear dynamic microwave losses of epitaxial hts films. *IEEE transactions on applied superconductivity*, 7(2):1236–1239, 1997.

[14] Karl P Horn, Meenu Upadhyay, Baruch Margulis, Daniel M Reich, Edvardas Narevicius, Markus Meuwly, and Christiane P Koch. Feshbach resonances in cold collisions as a benchmark for state of the art ab initio theory. *arXiv preprint arXiv:2408.13197*, 2024.

[15] M. A. Kuzovnikov et al. High-pressure synthesis and neutron scattering study of tantalum hydride tah.(5) and a tantalum polymorph with a15-type structure. *Physical Review B*, 110(18):184113, Nov. 2024.

[16] M Eisterer, A Bodenseher, and R Unterrainer. Universal degradation of high-temperature superconductors due to impurity scattering: predicting the performance loss in fusion magnets. *arXiv preprint arXiv:2409.01376*, 2024.

[17] Xie, T., Huo, M., Ni, X., Shen, F., Huang, X., Sun, H., ... & Wang, M. (2024). Neutron Scattering Studies on the High-T_c Superconductor $Li_3Ni_2O_{7-\delta}$ at Ambient Pressure. *arXiv preprint arXiv:2401.12635*.

[18] Murayama, Y. (1980). Theory of scattering in a superconducting state. *Physica A: Statistical Mechanics and its Applications*, *102*(3), 447-469.

[19] D. F. Besch. Thermal properties. *Microelectronics, Second Edition*, 39(1):2–1–2–8, 2005.

[20] F Pistolesi and Ph Nozieres. Superconductivity with hard-core repulsion: Bcs-bose crossover and s-/d-

wave competition. *Physical Review B*, 66(5):054501, 2002.

[21] H He, Y Sidis, Ph Bourges, GD Gu, A Ivanov, N Koshizuka, B Liang, CT Lin, LP Regnault, E Schoenherr, et al. Resonant spin excitation in an overdoped high temperature superconductor. *Physical Review Letters*, 86(8):1610, 2001.

[22] A. Ghirri, C. Bonizzoni, M. Maksutoglu, and M. Affronte. Interplay between magnetism and superconductivity in a hybrid magnon-photon bilayer system. *Physical Review Applied*, 22(3), September 2024.

[23] Rosa, F., Martinelli, L., Krieger, G., Braicovich, L., Brookes, N. B., Merzoni, G.,& Ghiringhelli, G. (2024). Spin excitations in $Nd_{1-x}Sr_xNiO_2$ and $YBa_2Cu_3O_{7-\delta}$: The influence of Hubbard U. *Physical Review B*, *110*(22), 224431.

[24] G. Merzoni, L. Martinelli, L. Braicovich, and N. Bontemps. Charge response function probed by resonant inelastic x-ray scattering: Signature of electronic gaps. *Physical Review B*, 109(184506), 2024.

[25] R. Coldea, S. M. Hayden, G. Aeppli, T. G. Perring, C. D. Frost, T. E. Mason, S.-W. Cheong, and Z. Fisk. Spin waves and electronic interactions in la_2cuo_4. *Physical Review Letters*, 86(23):5377–5380, 2001.

[26] J. M. Tranquada, H. Woo, T. G. Perring, H. Goka, G. D. Gu, G. Xu, M. Fujita, and K. Yamada. Quantum magnetic excitations from stripes in copper oxide superconductors. *Nature*, 429(6991):534–538, 2004.

[27] T. Miyatake, Y. Wako, R. Abe, S. Tsukamoto, and M. Uehara. Neutron diffraction study of layered nickelates $Pr_4Ni_{3-x}Co_xO_8$ for high-temperature superconductor candidate. *Journal of the Physical Society of Japan*, 93(2), February 2024.

[28] M. Ma et al. Ferromagnetic interlayer coupling in superconductors revealed by inelastic neutron scattering. *Physical Review B*, 110(174503), 2024.

[29] Griffin Heier and Sergey Y. Savrasov. Calculations of spin fluctuation spectral functions $\alpha^2 f$ in high-temperature superconducting cuprates. *arXiv preprint arXiv:2411.06537*, 2024.

[30] I. A. Zaluzhnyy et al. Structural changes in $YBa_2Cu_3O_7$ thin films modified with he+-focused ion beam for high-temperature superconductive nanoelectronics. *ACS Applied Nano Materials*, 7(14):15943–15949, July 2024.

[31] U. Oji, A. Hilger, I. Manke, C. Foerster, and R. C. Maier. Spatial 3d correlation of flux pinning with porosity distribution in $YBa_2Cu_3O_7$ − using tensorial neutron tomography. *Materials Today*, 2024.

[32] D. Gardew. High-temperature superconductors, 2024. Accessed: Dec. 04, 2024.

[33] Jan Brinckmann and Patrick A Lee. Renormalized mean-field theory of neutron scattering in cuprate superconductors. *Physical Review B*, 65(1):014502, 2001.

[34] Mingwei Ma, Philippe Bourges, Yvan Sidis, Yang Xu, Shiyan Li, Biaoyan Hu, Jiarui Li, Fa Wang, and Yuan Li. Prominent role of spin-orbit coupling in fese revealed by inelastic neutron scattering. *Physical Review X*, 7(2):021025, 2017.

[35] EV Antipov, AM Abakumov, VL Aksenov, AM Balagurov, SN Putilin, and MG Rozova. Neutron powder-diffraction studies of superconducting oxygenated and fluorinated hg-1201 phases. *Physica B: Condensed Matter*, 241:773–779, 1997.

[36] Jiakui K Wang, Liang L Zhao, Quan Yin, G Kotliar, MS Kim, MC Aronson, and E Morosan. Layered transition-metal pnictide srmnbi 2 with metallic blocking layer. *Physical Review B—Condensed Matter and Materials Physics*, 84(6):064428, 2011.

[37] A. Devitre, D. Fischer, K. Woller, et al. A facility for cryogenic ion irradiation and in situ characterization of rare-earth

barium copper oxide superconducting tapes. *Review of Scientific Instruments*, 95(6):063907, 2024. Accessed: Dec. 04, 2024.

[38] P. Monthoux, A. V. Balatsky, and D. Pines. Toward a theory of high-temperature superconductivity in the antiferromagnetically correlated cuprate oxides. *Physical Review Letters*, 67(22):3448–3451, 1991.

[39] D. J. Scalapino. A common thread: The pairing interaction for unconventional superconductors. *Reviews of Modern Physics*, 84(4):1383–1417, 2012.

[40] M. Eschrig. The effect of collective spin-1 excitations on electronic spectra in high-t_c superconductors. *Advances in Physics*, 55(1-2):47–183, 2006.